International Journal of Marine Engineering Innovation and Research, Vol. 10(4), Dec. 2025. 1162-1176
(pISSN: 2541-5972, eISSN: 2548-1479)

Experimental Investigation of the Municipal Solid Waste Characteristics for a Gasification-Based Waste-to-Energy Power Plants

Fazli Iqbal Pasha[1], Damora Rhakasywi[2*], Nicky Yongkimandalan[3], Regina N. Lumbantoruan[4], Z. H. Putty Fauthyda[5], F. Firmansyah[6], Anisa Rahmah Kusuma[7], Rizki Apriza[8]

(Received: 10 November 2025 / Revised: 14 November 2025 /Accepted: 16 November 2025 / Available Online: 1 December 2025)

***Abstract*— This study experimentally characterizes Municipal Solid Waste (MSW) feedstock to assess its suitability for gasification-based Waste-to-Energy (WtE) systems. Ten samples from different urban collection sites underwent thorough analysis using standardized ultimate and proximate methods, alongside bomb calorimetry on a dry basis, which helped to ensure the results accuracy. A strong positive correlation was observed between carbon and hydrogen content and gross calorific value, while oxygen, nitrogen, sulphur, and ash content exhibited a negative correlation with calorific potential. Notably, plastics and complex waste yielded the highest gross calorific values, around 30,000 kJ/kg and 31,600 kJ/kg, respectively, while high-ash content fractions recorded the lowest values at about 6,600 kJ/kg. The presence of volatile matter and fixed carbon positively impacts energy release, whereas ash dilutes fuel quality and increases heat absorption during combustion. The study suggests that pretreatment strategies, such as moisture reduction, ash fraction removal, and selective sorting for hydrocarbon-rich materials, effectively enhance fuel quality for gasification and reduce nitrogen and sulphur emission risks. The data reveal significant variability among different waste fractions, indicating that effective feedstock management and reactor design must address compositional heterogeneity to ensure reliable gasification performance.**

Keywords— Renewable Energy, Ultimate Analysis, Proximate Analysis, Gross Calorific Value, Municipal Solid Waste Sampling.

**Corresponding Author: rhakasywi@upnvj.ac.id*

I. INTRODUCTION

As civilization develops with high levels of industrial productivity, global energy consumption continues to surge. According to the International Energy Agency (IEA), global energy consumption has increased by 2.1% per year over the past decade. In addition, population growth in certain areas, especially in urban areas that are not decentralized, has caused environmental damage due to a decrease in green open spaces, while carbon emissions continue to rise. Data from the Indonesian Central Bureau of Statistics (BPS) shows that the population density ratio in DKI Jakarta Province reached 16,165 people/km^2 in 2024, which contributed significantly to the increase in electricity demand and the decrease in green open space. As a result, carbon emissions have increased dramatically, reaching more than 600 million tons of CO_2 per year in Indonesia. Most of these emissions still come from fossil fuel power plants and transportation [1], [2].

Increased productivity and population centralization have driven the use of relatively cheap, high-power, and techno-economically efficient energy sources such as coal. As of 2023, the total realized power plant capacity in Indonesia reached 72,032.9 MW, consisting of 44,723.7 MW owned by State Electricity Company (PLN), 26,110.8 MW from private companies, and 1,198.4 MW from leased assets, as shown in Figure 1. Most of these power plants are coal-fired steam power plants, which contribute around 52.2% of the total national electricity generation capacity, followed by gas power plants at around 27.73%, diesel power plants at around 5.67%, hydroelectric power plants at around 8.02%, geothermal power plants at around 3.5%, oil/gas steam power plants at around 2.2%, and the remaining percentage comes from renewable energy power plants [3].

The aggregate percentage of energy capacity generated by coal-fired power plants exhibited an average annual increase of 1.91% from 2015 to 2023. This sustained escalation in coal utilization and mining can precipitate a surge in the generation of air pollutants, including sulphur oxides (SO_X), nitrogen oxides (NO_X), and particulate matter with a diameter of 2.5

Fazli Iqbal Pasha, Departement of Mechanical Engineering, Universitas Pembangunan Nasional Veteran Jakarta, Jakarta, 12450, Indonesia. E-mail: fazlipasha429@gmail.com
Damora Rhakasywi, Departement of Mechanical Engineering, Universitas Pembangunan Nasional Veteran Jakarta, Jakarta, 12450, Indonesia. E-mail: rhakasywi@upnvj.ac.id
Nicky Yongkimandalan, Departement of Mechanical Engineering, Universitas Pembangunan Nasional Veteran Jakarta, Jakarta, 12450, Indonesia. E-mail: nickyyongkimandalan@gmail.com
Regina N. Lumbantoruan, Departement of Mechanical Engineering, Universitas Pembangunan Nasional Veteran Jakarta, Jakarta, 12450, Indonesia. E-mail: reginatalindah17@gmail.com
Z. H. Putty Fauthyda, Departement of Mechanical Engineering, Universitas Pembangunan Nasional Veteran Jakarta, Jakarta, 12450, Indonesia. E-mail: puttyfauthyda@gmail.com
F. Firmansyah, Departement of Mechanical Engineering, Universitas Pembangunan Nasional Veteran Jakarta, Jakarta, 12450, Indonesia. E-mail: firmansyah090504@gmail.com
Anisa Rahmah Kusuma, Departement of Mechanical Engineering, Universitas Pembangunan Nasional Veteran Jakarta, Jakarta, 12450, Indonesia. E-mail: anisarhmhksm@gmail.com
Rizki Apriza, Departement of Mechanical Engineering, Universitas Pembangunan Nasional Veteran Jakarta, Jakarta, 12450, Indonesia. E-mail: rizkiapriza5@gmail.com

micrometers or less (PM2.5). The process of deforestation that occurs in conjunction with mining activities has the potential to inflict irreparable ecological damage [3].

concomitant with increased waste production. The dynamics of urbanization and economic growth have resulted in a marked increase in the volume of Municipal Solid Waste (MSW), thereby underscoring the pressing need for the development and implementation of effective waste management infrastructure. In developed countries, landfills frequently employ the use of thick plastic to impede the leakage of contaminants into the environment. Concurrently, developing countries frequently possess open landfills, which facilitate the facile dispersal of plastic into the environment. In the United States, it is estimated that 0.98-1.26 million metric tons of plastic, representing 2.33-2.99% of the total plastic waste, escapes into the environment. Furthermore, substantial quantities of plastic debris are released into the environment during natural disasters. By the year 2030, the annual global contribution of plastic to the world's oceans is projected to reach 58.4 million tons. In Indonesia, approximately 65 million tons of waste is produced per year, of which 69% is disposed of in 94 landfills, only 7% is recycled, and approximately 24% of the remainder is illegally dumped into the environment. The predominant proportion of this waste is designated as MSW, which possesses the capacity to induce soil and water contamination, in addition to greenhouse gas emissions, including methane, emanating from anaerobic decomposition processes within landfills [4], [5], [6].

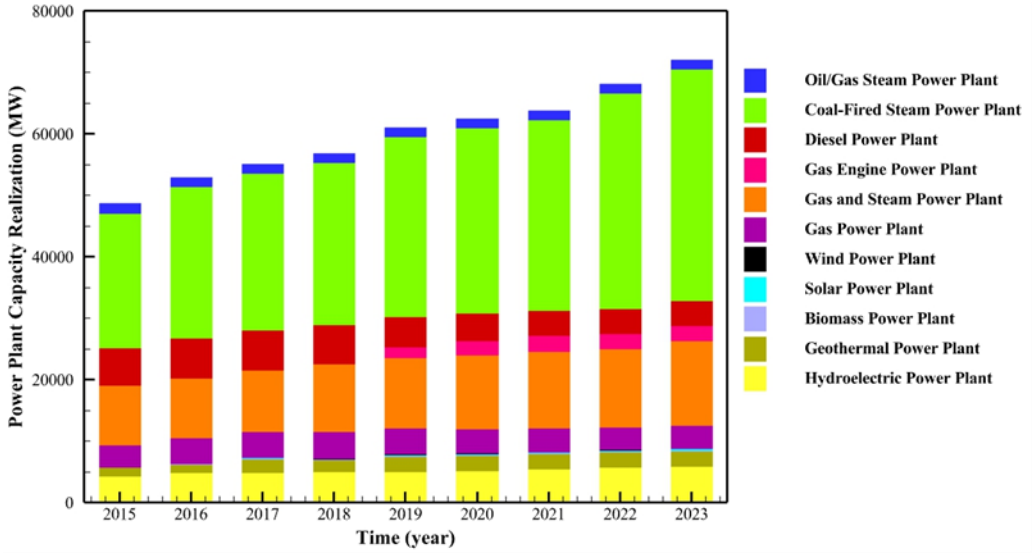

Figure. 1. Power Plant Capacity Realization [3].

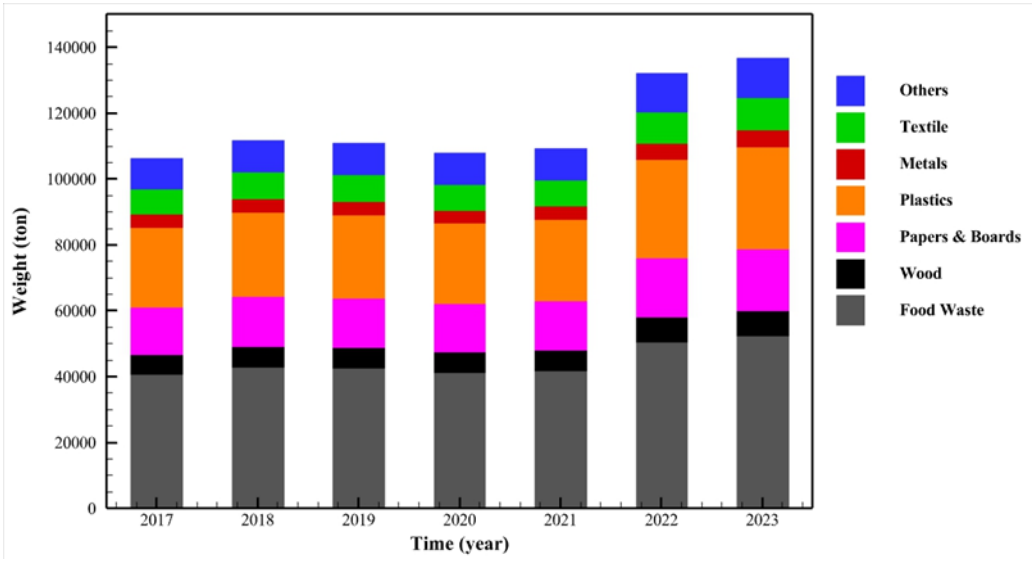

Figure. 2. Recapitulation of Waste Weighing in Surakarta City [7], [8].

A summary of waste weighing data from the National Waste Management Information System (SIPSN) and SENADA 2024 proceedings, as presented in Figure 2, reveals a notable increase in waste production in Surakarta City from 2017 to 2023, with a total of 30,487.36 tons of waste generated. The mass distribution by fraction in 2023 demonstrates the preeminence of the organic fraction, which constitutes 38.18% of the total, amounting to approximately 52,217.34 tons. This is followed by the plastic fraction, which accounts for

22.73% of the total, equivalent to around 31,086 tons. The total weight of the paper and cardboard was 13.64%, which is equivalent to approximately 18,654.91 tons. The textile fraction was reported to be 7.27%, or approximately 9,942.9 tons, while wood contributed 5.64%, or around 7,713.61 tons, and metals 3.64%, or around 4,978.29 tons. This composition exhibits the characteristics of waste streams, with a predominance of organic materials and a significant proportion of readily separable inorganic materials, such as plastic and paper [7], [8].

Waste-to-Energy (WtE) technology offers a promising solution to address two issues simultaneously: the need for clean energy and waste management. One of the methods that has been developed is gasification, a thermochemical process that converts waste into synthetic gas (syngas) that can be used as fuel for WtE power plants. This system has the advantage of lower emissions compared to direct combustion such as incineration, as well as higher energy efficiency, especially when operating conditions are optimally controlled. Studies conducted in 2021 and 2022 have explained that WtE Power Plants are a sustainable solution for waste management, contributing to low-carbon and circular economy values. Both studies emphasize the importance of evaluating thermochemical energy conversion technologies by considering technical, economic, and environmental aspects. The results show that the thermochemical gasification approach is a better option in terms of emissions, capital costs, quality, electricity production, and remains competitive in terms of capacity [9], [10].

Several other recent studies have also shown that thermochemical approaches such as pyrolysis and gasification are promising methods for recycling plastic waste, particularly polyolefins, into high-value products such as light olefins and synthetic gas. Research shows that catalytic pyrolysis can produce up to 85% C2–C4 olefins under laboratory conditions using pure polyolefins, while thermal pyrolysis and gasification are considered superior in terms of process robustness, feedstock flexibility, and energy conversion efficiency. However, all three studies emphasize the importance of reactor design optimization, secondary reaction control, and understanding chemical mechanisms to maximize desired product yields and reduce tar and coke formation. The complexity of solid plastic waste composition and the variability of additive and contaminant mixtures pose significant challenges that require further experimental approaches and more accurate reaction kinetics modeling. Therefore, future research will focus on developing selective catalysts, more precise raw material characterization techniques, and integrating experimental data-based reactor models to achieve better economic and environmental efficiency in circular economy schemes [11], [12], [13].

The employment of thermochemical gasification methods has yielded substantial advancements in environmental sustainability, notably through the effective management of waste and the generation of novel renewable energy sources. This objective is consistent with Government Regulation No. 79 of 2014 concerning National Energy Policy, which prioritizes the utilization of renewable energy sources with the aim of reducing the reliance on fossil-based energy and decreasing the economic value of carbon [14]. However, despite the minimal carbon emissions of this method, researchers face challenges in utilizing more precise MSW characterization techniques due to the variation in MSW characteristics, which complicates the prediction of gasification performance. Consequently, experimental investigation grounded in field conditions is imperative to attain a more precise comprehension of the relationship between these variables. This is a pivotal factor in the success of renewable energy sources that are both efficient and environmentally friendly. The objective of this study is to conduct an experimental investigation of WtE facilities using real data from the field. The primary objective of this study is to examine the correlation between the elemental composition and the thermal characteristics of MSW, as well as its calorific value. The findings of this study are anticipated to facilitate the development of more reliable and efficient WtE systems in the future.

II. Method

A. Time and Location

This study was conducted over the course of twenty weeks, commencing on February 1, 2025, with a preliminary literature review that sought to establish the theoretical underpinnings and relevant supporting data pertinent to the research subject. The subsequent stage was sampling, which was conducted from February 9 to 17, 2025, in Surakarta City, Central Java, Indonesia, between 9:00 and 14:00 Western Indonesian Time (2:00 to 7:00 UTC) to ensure that the environmental conditions and sample characteristics were maintained. Subsequent to this procedure, a series of sample feasibility tests will be conducted until March 28, 2025, with the objective of ensuring that the samples meet the criteria for representativeness and adhere to the standards established by the ASTM. Subsequent laboratory testing is scheduled to continue until April 25, 2025, at the Mineral and Coal Business Unit of PT. Surveyor Indonesia, situated at Jenderal Gatot Subroto Street, Central Jakarta, Indonesia, is responsible for the acquisition of quantitative data. The subsequent stage, from the thirteenth to the fifteenth week, centered on the processing of the test results and statistical analysis at the campus of the Universitas Pembangunan Nasional Veteran Jakarta, RS. Fatmawati Raya Street, South Jakarta, Indonesia. During the past five weeks, the emphasis was placed on the formulation of hypotheses and the systematic and structured documentation of research results.

B. Feedstock Sampling

In principle, measurement involves taking a large number of samples that represent the overall characteristics of MSW. The selection of a sample is informed by the recognition that each road, each district, each area, and each weather condition possess unique characteristics. This acknowledgment necessitates a meticulous and iterative process in the selection of the sample, which is characterized by frequent reversals and

repetitive procedures. In practice, this type of sampling would not be feasible to carry out in a short period of time and would have to rely on random sampling at landfills and incoming trucks. Consequently, the sampling procedure entails the collection and examination of 10 samples, which collectively encompass all the characteristics with measurements in accordance with ASTM standards. This approach is employed to ascertain the parameters that exert an influence on the thermal characteristics of MSW. The parameters that are taken into consideration include moisture, density, and size.

Sampling was carried out in stages to ensure the representativeness and traceability of the samples. The procedure began with the collection of one ton of samples from trucks and landfills, which were then placed on plastic nets to facilitate handling and visual inspection, as shown in Figure 3. All bags are opened and their contents separated so that waste pieces larger than 40 × 40 cm are taken separately to be weighed, identified, and documented as preliminary material quality data, while the remaining smaller waste is stored for the next step [15], [16].

The remaining contents of one package are mixed with the remaining contents of the next package using a mechanical shovel to ensure that the material composition is evenly distributed before being poured into four large boxes. Of these four boxes, the two boxes in the diagonal position are selected as material for the next package while the other two boxes are returned to the facility for storage or reprocessing [16], [17], [18]. This process can be seen in Figure 4.

Figure. 3. Waste Sorting Based on Size.

Figure. 4. Package (Sub-Sample) Mixing.

During the mixing process, the division into four boxes and the selection of two diagonal boxes are repeated alternately until the package being processed is exhausted, so that the procedure produces a representative subsample of the initial package. The same cycle is then applied sequentially between packages until the total weight of the final sample reaches approximately 100 kg, which becomes the working sample. Throughout the entire procedure, detailed records and documentation are kept of the collection, separation, weighing, and selection of boxes to ensure the traceability and validity of the sample [19]. Once the working sample was obtained, its moisture content, density, and size were measured.

The procedure for determining the moisture content in waste entails the following steps. First, the sample is spread on a tray measuring 20 centimeters in height. Then, the tray is placed in an oven equipped with a fan set to 90℃ at normal atmospheric pressure. The drying process is continued until a constant weight is achieved, with the criterion of less than 1% weight variation between consecutive weighing conducted at half-hour intervals. The measurement of moisture content, expressed as a percentage of the total mass (%), was conducted by employing the scales depicted in Figure 5 (a) and subsequently calculated using the following Equation (1), where W_{humid} signifies the initial (wet) weight in kilograms and W_{dry} denotes the final (dry) weight in kilograms.

Figure. 5. Density and Size Measuring Instrument.

$$MC = \frac{W_{humid} - W_{dry}}{W_{humid}} \times 100\% \quad (1)$$

The density of mixed waste is determined by weighing an empty 200-liter barrel before and after it is filled with uncompacted waste. The density (ρ_{MSW}) is calculated using Equation (2), where W_{gross} indicates the gross weight (inclusive of waste) in kilograms and W_{barrel} is the weight of the empty barrel in kilograms. The effective identification of dry waste is imperative for ensuring safety, hygiene, and improving working conditions. To this end, each sample, with a mean mass of approximately 100 kilograms, must undergo a drying procedure. The methodology entails the sorting of materials based on their size, utilizing a sorting table accompanied by three perforated plates and a recovery box that lacks a ground opening. The sorting table is designed with apertures measuring 100 mm, 20 mm, and 8 mm, thereby facilitating the efficient separation of materials, as illustrated in Figure 5 (b).

$$\rho_{MSW} = \frac{W_{gross} - W_{barel}}{200} \quad (2)$$

C. Laboratory Test

The objective of the laboratory testing conducted in this study was to obtain detailed physical and chemical characterization data from MSW samples and biochar products. The testing regimen encompassed several analyses: ultimate analysis, which measured the elemental composition including carbon (C), hydrogen (H), nitrogen (N), sulphur (S), and oxygen (O); proximate analysis, assessing moisture content (MC), volatile matter (VM), fixed carbon (FC), and ash content; and the evaluation of gross calorific value (GCV), all performed in compliance with relevant standards. This comprehensive approach guarantees a comprehensive understanding of the composition and energy potential of the examined materials.

In the case of ultimate analysis, the measurements in a combustion furnace at a specific temperature, as shown in Table 2, enable the quantification of elemental components in a sample using a CHNSO analyzer (see Figure 6 (a)). The combustion process converts carbon to carbon dioxide (CO_2), hydrogen to water (H_2O), and nitrogen to nitrogen (N2). Subsequent to the combustion process, the gases are purified and detected using a thermal conductivity detector (TCD). The recalculation of carbon, hydrogen, and nitrogen concentrations as percentages is based on the standards outlined in ASTM D5373-16 [20]. The presence of sulphur is determined through the use of infrared absorption detection during the process of sample combustion in a pure oxygen flow. This method involves the oxidation of sulphur to SO_2. The concentration of sulphur is then measured in proportion to the infrared absorption, in accordance with the standards outlined in ASTM D4239-18 [21], [22], [23]. Oxygen analysis is calculated indirectly from the remaining sample using Equation (3). An exhaustive list of the ultimate analysis parameters can be found in Table 1.

$$O = 100\% - \left(C + H + N + S + Ash\right) \quad (3)$$

The results of the ultimate analysis form the basis for the proximate analysis stage, which focuses on the operational characteristics of fuel, including moisture content, volatile matter, ash, and fixed carbon. These two analyses complement each other, the ultimate analysis describes the chemical composition, while the proximate analysis assesses how the fuel reacts to heating and combustion. The proximate analysis process commences with the determination of moisture content. This is achieved through a drying method at 90°C until a constant weight is attained, a process that takes approximately 24 hours. This procedure is in accordance with the ASTM D3173M-17 standard. The discrepancy between the initial and final weights is expressed as a percentage of moisture content to standardize the results on a dry basis. The presence of high moisture content in fuel has been shown to reduce its calorific value and efficiency. This is due to the fact that a portion of the combustion energy is allocated to the process of water evaporation [24], [25], [26], [27], [28].

The subsequent stage in the analysis is the determination of volatile matter and ash content. The quantification of volatile matter is conducted in accordance with the provisions stipulated in ASTM D3175-18. This procedure is employed to ascertain the proportion of gas released at elevated temperatures. The resultant data provides insights into the propensity for ignition and the stability of combustion of the fuel [24],

[29], [30], [31], [32]. Meanwhile, ash is the inorganic residue remaining after the material is completely burned at high temperatures. It consists of minerals such as silica, alumina, and iron oxide. The measurement of ash is conducted in accordance with the standard outlined in ASTM D3174-12. The ash value is a critical component in the evaluation of fuel quality, as it plays a pivotal role in determining the propensity for deposit formation in combustion equipment. Furthermore, the ash value is instrumental in quantifying the amount of non-combustible residue that necessitates management [25], [29], [33].

The final parameters are fixed carbon and gross calorific value, which is the fraction of solid carbon remaining after volatiles are released [30], [34]. The gross calorific value is calculated based on the ASTM D3172-13 method. A high fixed carbon content is indicative of optimal fuel quality, as it is the primary contributor to the calorific value. The gross calorific value is subsequently determined through the utilization of a bomb calorimeter, in accordance with the standards outlined in ASTM D5865/D5865M-19 (see Figure 6 (b)). The proximate analysis results are reported in mass percent on a dry basis to facilitate inter-sample comparisons and corrected calorific value calculations, as presented in Table 1. All testing procedures are supplemented with quality control measures, including instrument calibration, duplicate analysis, blanks, and the use of reference standards. These measures ensure the reliability and accuracy of laboratory results [24], [29], [30], [31], [32].

Table 2 provides a comprehensive documentation of the boundary conditions that were utilized in a series of laboratory tests, the purpose of which was to simulate the conditions associated with the gasification process. These parameters are critical for predicting the elemental composition and thermal characteristics at high temperatures. These instruments facilitate the assessment of the risk of ash formation post-gasification, thereby ensuring the applicability of laboratory findings to the operational and maintenance conditions of WtE power plants. The utilization of these parameters enables researchers to effectively bridge the gap between laboratory data and real-world applications in gasification technology.

D. Statistical Test

All experimental data and subsequent derivative values are processed according to a documented workflow. This ensures reproducibility and validity of inferences. The process of statistical testing commences with the conversion of the standardized reporting basis to a dry basis. Subsequently, the dataset undergoes a process of refinement, encompassing the management of missing data, the identification and resolution of duplicates, and the examination of outliers. This preparatory phase is followed by an assessment of the dataset's normality. The software utilized for this purpose includes IBM SPSS, Microsoft Excel, and Tecplot 360.

The Shapiro-Wilk test is a statistical method for testing the null hypothesis that a sample comes from a normal distribution. The test statistic W is formed from a linear combination of ordered observation values (order statistics) compared to the sample variance, so this test evaluates the degree of data conformity to linearity on a normal probability plot. Mathematically, W is expressed as the ratio of the sum of squares of a linear combination of ordered observations to the sum of squares of deviations from the mean, as shown in Equation (4). Where the coefficient ai depends on the sample size n and is obtained from the expected value and covariance of the normal order statistics. The value of W ranges up to 1, with values close to 1 indicating conformity with normality, while small values indicate deviation from normality.

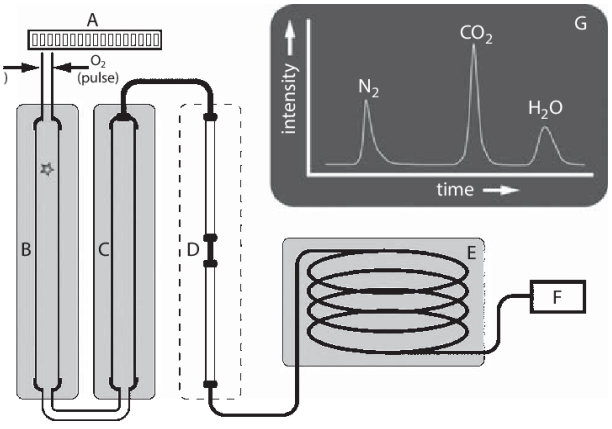

(a) CHNSO Analyzer Design of Experiment (DoE) [39].

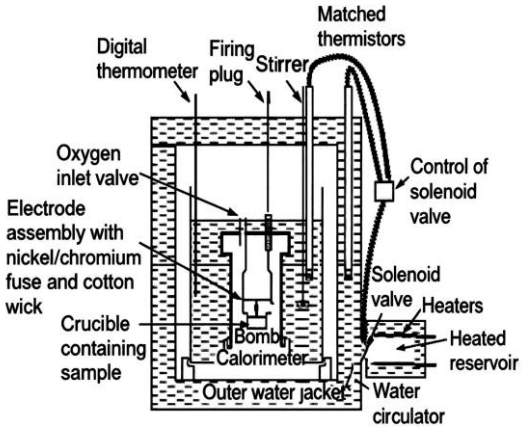

(b) Bomb Calorimeter Design of Experiment (DoE) [40].

Figure. 6. Laboratory Measuring Instrument.

$$W = \frac{\left[\sum_{i=1}^{n} a_i y_i\right]^2}{\sum_{i=1}^{n}\left(y_i - \bar{y}\right)^2} \quad (4)$$

Due to its construction, Shapiro-Wilk is invariant to shifts in location and scale, and has been shown to have good power, especially in small to medium samples, for detecting asymmetry and skewness compared to other tests such as Kolmogorov-Smirnov or chi-square tests. Therefore, this test is widely recommended as the

primary normality test in experimental studies with limited sample sizes

In practice, performing the Shapiro-Wilk normality test involves sorting the data, calculating W, and testing for significance by comparing the p-value to the specified α level. This test should be used in conjunction with graphical inspections such as Q-Q plots and outlier checks because W is sensitive to extreme observations that may be measurement artifacts. If W indicates a rejection of normality (p-value < α), a reasonable follow-up is to consider data transformation, use nonparametric methods, or employ robust procedures that do not assume normality. When reporting results, include the W statistic value, sample size n, and p-value, as well as any follow-up actions taken if normality is violated [35].

TABLE 1.
ULTIMATE AND PROXIMATE ANALYSIS PARAMETERS

Parameter		Unit	Method
Ultimate Analysis	Total Carbon (C)	wt%	ASTMD5373-16
	Total Hydrogen (H)	wt%	
	Total Nitrogen (N)	wt%	
	Total Sulphur (S)	wt%	ASTM D4239-18
	Total Oxygen (O)	wt%	By Different
Proximate Analysis	Moisture Content (MC)	wt%	ASTM D3173M-17
	Ash Content	wt%	ASTM D3174-12
	Volatile Matter (VM)	wt%	ASTM D3175-18
	Fixed Carbon (FC)	wt%	ASTM D3172-13
	Gross Calorific Value (GCV)	kJ/kg	ASTM D5865/D5865M-19

TABLE 2.
BOUNDARY CONDITIONS

Parameter		Value	Unit	Method
Reduction Parameter (Ultimate Analysis)	Initial Deformation Temp.	1180 – 1310	°C	ASTM D1857M-18
	Spherical Temp.	1200 – 1330	°C	
	Hemispherical Temp.	1200 – 1340	°C	
	Fluid Temp.	1210 – 1360	°C	
Drying Parameter (Proximate Analysis)	Oven Temp.	90	°C	ASTM D3173M-17
	Residence Time	24	Hours	

Subsequent to the cleansing of the dataset, the residual normality was examined through the utilization of Q-Q plots and the Shapiro-Wilk method, in order to ascertain the viability of employing parametric tests. The results of the Q-Q plot normality test, as depicted in Figure 7, indicate that the data follows a normal distribution.

The normality test was subsequently conducted using the Shapiro-Wilk test with a 95% confidence interval and a significance level of $\alpha = 0.05$. Two hypotheses were put forward for consideration. If the p-value is greater than or equal to α, then the null hypothesis, H_0, is accepted, meaning that the data is normally distributed. If the p- value is less than α, then the alternative hypothesis, H_1, is accepted, meaning that the data is not normally distributed. As demonstrated in Table 3, the empirical data demonstrate that the p-value exceeds the level of significance (α) for all parameters within each group. Consequently, the null hypothesis is to be accepted.

Levene's test is a robust method for testing the null hypothesis that the variances between groups are equal. The fundamental premise of this approach entails the conversion of the issue of testing variances into one of comparing the means of the absolute deviations from the central tendency measures of each group [36].

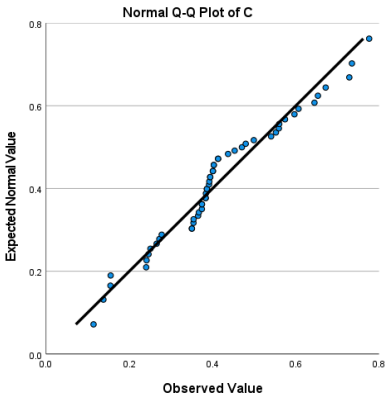

(a) Q-Q Plot of Carbon.

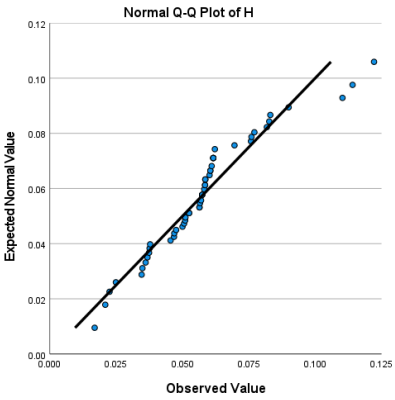

(b) Q-Q Plot of Hydrogen.

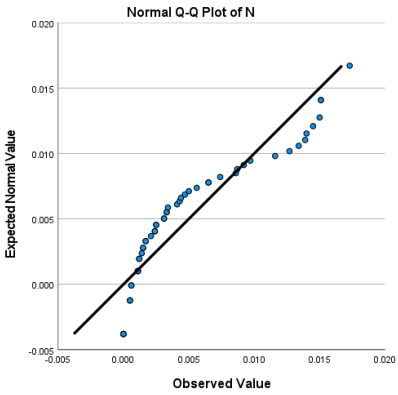

(c) Q-Q Plot of Nitrogen.

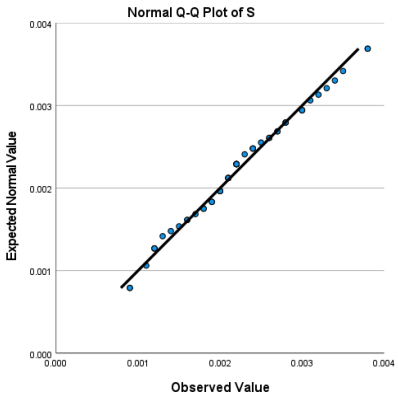

(d) Q-Q Plot of Sulphur.

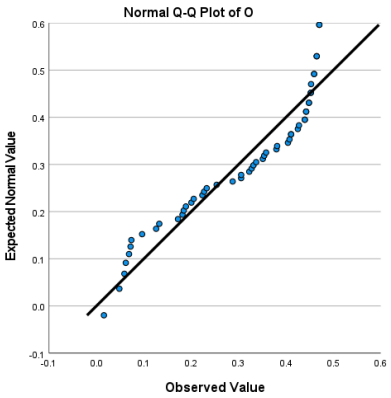

(e) Q-Q Plot of Oxygen.

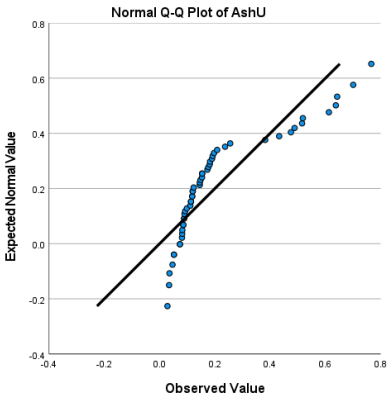

(f) Q-Q Plot of Ash (Ultimate).

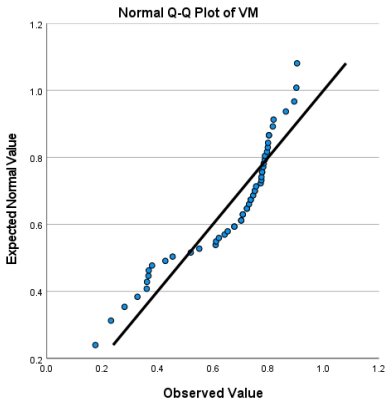

(g) Q-Q Plot of Volatile Matter.

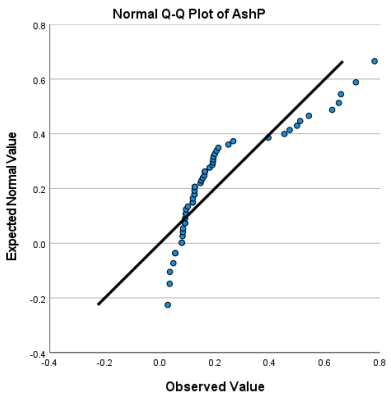

(h) Q-Q Plot of Ash (Proximate).

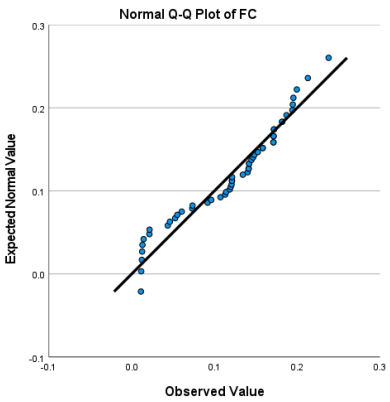

(i) Q-Q Plot of Fixed Carbon.

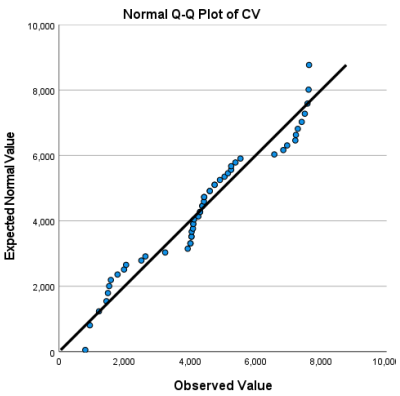

(j) Q-Q Plot of Gross Calorific Value.

Figure. 7. Q-Q Plot of Ultimate and Proximate Analysis.

Subsequent to the distribution of the data in the Q-Q plot and the execution of the Shapiro-Wilk normality test, statistical analysis progresses to the stage of testing for variance homogeneity using Levene to determine the feasibility of employing parametric tests. The statistical analysis of the test results indicates that the significance value is less than 0.05 for all test variables with the exception of fixed carbon, for which the p-value is approximately 0.076. Consequently, the prevailing hypothesis, H_1, states that the data is not homogeneous. The Levene homogeneity test, based on the mean, is presented in Table 4.

TABLE 3.
SHAPIRO-WILK NORMALITY TEST OF ULTIMATE AND PROXIMATE ANALYSIS

Group (Variance)	P-Value									
	C	H	N	S	O	Ash(U)	VM	Ash(P)	FC	GCV
Organics	0.40	0.23	0.16	0.29	1.00	0.06	0.16	0.07	0.05	0.11
Papers	0.95	0.30	0.59	0.94	0.25	0.95	1.00	0.93	0.38	0.77
Board	0.95	0.30	0.59	0.94	0.25	0.95	1.00	0.93	0.38	0.77
Complex Waste	0.28	0.15	0.14	0.27	0.37	0.67	0.12	0.62	0.70	0.25
Textile	0.42	0.12	0.51	0.40	0.21	0.12	0.78	0.15	0.19	0.92
Plastics	0.23	0.61	0.27	0.25	0.15	0.83	0.45	0.78	0.30	0.42
Unclassified Combustible Waste	0.07	0.14	0.11	0.50	0.39	0.12	0.68	0.41	0.20	0.77
Small (8-20 mm)	0.10	0.06	0.83	0.42	0.07	0.07	0.69	0.26	0.64	0.37

TABLE 4.
LEVENE'S HOMOGENEITY TEST OF ULTIMATE AND PROXIMATE ANALYSIS

Variable	P-Value
Carbon (C)	0.00151346
Hydrogen (H)	0.00154823
Nitrogen (N)	0.00000023
Sulphur (S)	0.00966243
Oxygen (O)	0.03909681
Ash Content (Ultimate)	0.00011584
Volatile Matter (VM)	0.00222045
Ash Content (Proximate)	0.00016044
Fixed Carbon (FC)	0.07639639
Gross Calorific Value (GCV)	0.00000064

TABLE 5.
ROBUST WELCH ANOVA AND BROWN-FORSYTHE TESTS OF ULTIMATE AND PROXIMATE ANALYSIS

Variable	P-Value	
	Welch ANOVA	Brown-Forsythe
Carbon (C)	< 0.00000001	< 0.00000001
Hydrogen (H)	< 0.00000001	< 0.00000001
Nitrogen (N)	< 0.00000001	< 0.00000001
Sulphur (S)	0.36558384	0.61305673
Oxygen (O)	< 0.00000001	< 0.00000001
Ash Content (Ultimate)	< 0.00000001	< 0.00000001
Volatile Matter (VM)	< 0.00000001	< 0.00000001
Ash Content (Proximate)	< 0.00000001	< 0.00000001
Fixed Carbon (FC)	< 0.00000001	< 0.00000001
Gross Calorific Value (GCV)	< 0.00000001	< 0.00000001

In instances where the assumptions of one-way ANOVA, particularly the equal variances assumption, are not met, Welch ANOVA and Brown Forsythe tests serve as alternative statistical methods. The Welch ANOVA is a statistical method that addresses the challenges posed by unequal variances and imbalanced sample sizes. It does so by calculating weighted group means, thereby enhancing the reliability of p-values

through the Welch Satterthwaite approximation for degrees of freedom [37]. In contrast, the Brown Forsythe test improves upon the Levene test by focusing on absolute deviations and suggests using the median or the trimmed mean rather than the mean. This enhancement in robustness is particularly relevant in the presence of non-normality and outliers. This enhanced precision leads to more accurate determinations of significance levels in skewed distributions in comparison to conventional tests such as the F-test or Bartlett test [38].

The criteria for hypothesis testing are as follows: if the p-value is greater than α, the null hypothesis (H_0) of no significant difference between group means is accepted, if the p-value is less than α, the alternative hypothesis (H_1) is accepted. The Welch ANOVA was selected due to its capacity to accommodate differing variances across groups. The methodological results indicate that the majority of variables are not statistically significant, with the notable exception of the sulphur variable, which exhibited significance in Welch ANOVA (p-value ≈ 0.366) and Brown Forsythe test (p-value ≈ 0.613). This finding supports the acceptance of H_1, indicating a significant difference in means between groups. The outcomes of the robust tests are summarized in Table 5.

III. Results and Discussion

A. Sampling Results

The dry sample weight indicated in Table 6 signifies substantial moisture content, which encompasses non-combustible materials such as metal and glass that do not contribute to calorific value. Normalization has been demonstrated to enhance energy potential by eliminating non-calorific elements and increasing the proportion of usable combustibles, such as plastic and paper. Despite the prevalence of organic waste, its moisture content compromises its heat efficiency in comparison to plastics. Accurate energy analysis necessitates the incorporation of both raw and normalized calorific values based on dry mass. This approach is imperative for ensuring the precision of process design and emissions calculations, particularly in the face of variability. Furthermore, MSW is categorized by mass fractions, as delineated in Table 7.

Table 6.
Weight and Moisture Content of each Sample

Measurement Parameters	Sample No.										Avg.	N.
	1	2	3	4	5	6	7	8	9	10		
Weight of Dry Sample (kg)	173	151	106	138	140	168	120	118	150	117	138.10	118.08
Moisture Content (%)	58.38	42.59	44.37	58.43	53.23	59.68	53.68	62.33	62.37	46.97	54.20	46.35

Table 7.
Classification of MSW based on Mass Fractions

MSW Classification	Sample No. (wt%)										Avg. (wt%)	N. (wt%)
	1	2	3	4	5	6	7	8	9	10		
Organics	36.86	29.99	24.89	34.08	22.07	30.40	25.98	48.66	37.68	27.11	31.77	37.16
Papers	5.96	5.74	3.78	2.65	6.90	8.99	13.67	6.37	2.14	5.95	6.22	7.27
Board	1.11	1.48	0.76	0.94	6.35	0.99	1.22	0.85	2.55	4.42	2.07	2.42
Complex Waste	17.53	11.85	15.58	13.76	9.68	8.80	5.94	7.18	8.15	14.59	11.30	13.22
Textile	2.19	10.45	4.05	4.88	8.61	6.75	12.25	4.75	8.38	1.22	6.35	7.43
Plastics	14.26	16.46	27.18	22.33	23.59	16.56	9.64	15.95	12.74	16.12	17.48	20.45
Unclassified Combustible Waste	5.61	6.01	0.63	2.23	1.59	2.16	1.01	1.08	2.23	14.38	3.69	4.32
Glass	1.46	2.58	6.26	1.13	1.77	1.89	1.08	1.44	4.73	0.00	2.23	-
Metal	0.76	0.00	0.95	0.00	0.55	0.00	0.00	0.00	0.92	2.45	0.56	-
Unclassified Uncombustible Waste	0.78	0.00	0.00	0.56	1.83	2.36	0.00	0.00	0.99	0.00	0.65	-
Special Waste	0.00	0.00	0.00	0.00	0.55	1.18	2.23	0.90	0.00	0.00	0.49	-
Small (8-20 mm)	6.11	5.93	7.80	6.97	6.57	7.38	9.35	5.85	7.97	2.21	6.61	7.74
Fines (<8 mm)	7.36	9.51	8.11	10.46	9.93	12.55	17.63	6.97	11.51	11.57	10.56	-

B. Ultimate Analysis

The ultimate analysis constitutes a comprehensive evaluation that reveals the mass fraction of elemental composition for each MSW category on a dry basis. The presentation of the data on a dry basis ensures that the comparisons made are not affected by the moisture content. This, in turn, facilitates more accurate interpretation of the energy. The subsequent table offers a comprehensive overview of the most promising categories for energy recovery and those that necessitate specialized treatment due to their ash content or emission-producing elements. Consequently, Table 8 offers a quantitative foundation for recommendations concerning pre-treatment sorting and energy conversion process design.

The data presented in Figure 8 indicates a discernible positive correlation between the carbon and hydrogen content and the gross calorific value of MSW fragments.

This suggests that as the proportion of carbon and hydrogen elements in MSW fragments increases, the gross calorific value produced also increases. The plastic and complex waste fractions are notable for their high carbon and hydrogen values, which contribute to their high gross calorific value. In contrast, the organic and small particle fractions exhibit low carbon and hydrogen content, resulting in the lowest gross calorific value. This relationship is consistent with the principle that hydrocarbon compounds store more energy per unit mass than wet or inorganic materials. Consequently, the elemental composition of these materials is a direct indicator of their energy potential. In practice, the focus of sorting for energy recovery purposes should prioritize the separation of plastics and high-hydrocarbon materials. Furthermore, the measurement of carbon and hydrogen elements as part of the raw material inventory before designing the energy conversion process is essential.

TABLE 8.
ULTIMATE ANALYSIS AND GROSS CALORIFIC VALUE

Category	Elemental Composition (wt%)						GCV (kJ/kg)
	C	H	N	S	O	Ash (U)	
Organics	35.610	4.836	1.215	0.219	33.089	25.031	13382.879
Papers	38.843	5.839	0.111	0.254	44.872	10.082	18104.381
Board	38.570	5.847	0.153	0.231	43.756	11.443	17906.940
Complex Waste	54.766	8.144	0.232	0.226	22.847	13.785	31588.693
Textile	50.336	5.293	0.317	0.227	37.539	6.289	21851.074
Plastics	74.680	11.553	0.127	0.170	5.290	8.180	30314.031
Unclassified Combustible Waste	65.683	7.630	0.470	0.277	6.091	19.849	28428.064
Small (8-20 mm)	20.156	2.972	1.107	0.191	16.041	59.533	6654.604

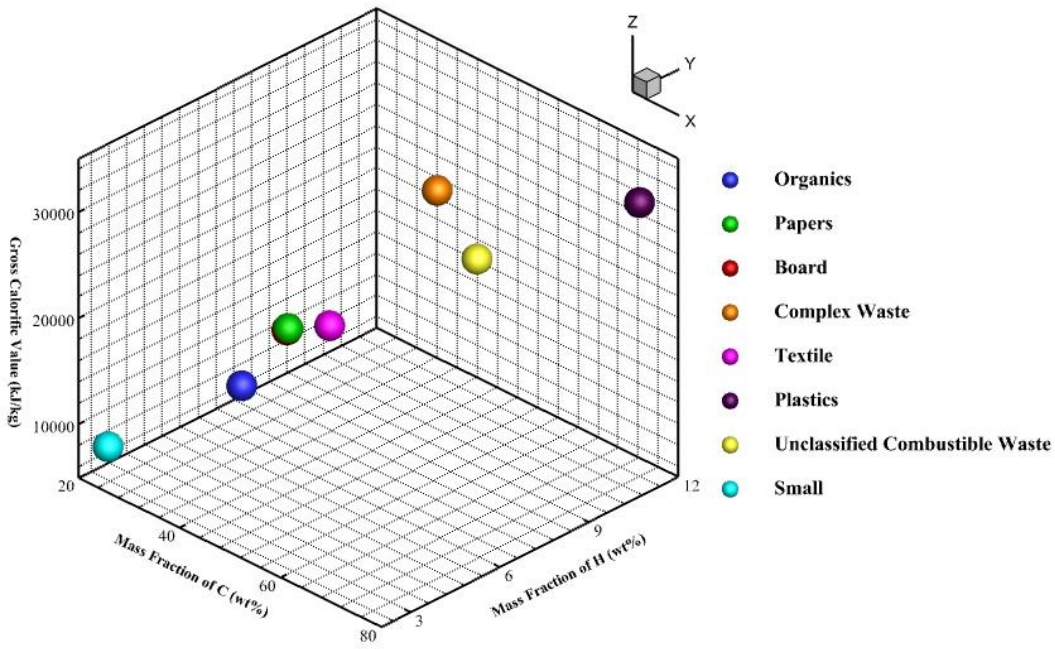

Figure. 8. Graph of Carbon and Hydrogen vs Gross Calorific Value.

As illustrated in Figure 9, there is an inverse correlation between the nitrogen mass fraction and the gross calorific value. This indicates that an increase in nitrogen content results in a decrease in calorific value. Conversely, the relationship between sulphur content and gross calorific value appears erratic, complicating predictions regarding energy potential. MSW categories characterized by elevated concentrations of nitrogen (N) and sulphur (S), particularly organic materials and small particulates, typically exhibit reduced calorific values. Conversely, plastics and hydrocarbon-rich materials exhibit reduced nitrogen and sulphur levels, contributing to their higher calorific values. The implications of significant nitrogen and sulphur presence extend beyond diminished energy potential, they also suggest increased risks of nitrogen oxides (NO_X) and sulphur oxides (SO_X) emissions during combustion processes. Consequently, any energy evaluation must encompass both the calorific value and the fractions of nitrogen and sulphur, thereby ensuring a comprehensive analysis of raw materials. This strategy is imperative for accurately estimating emission control requirements and selecting appropriate strategies for material separation or pretreatment before energy conversion processes.

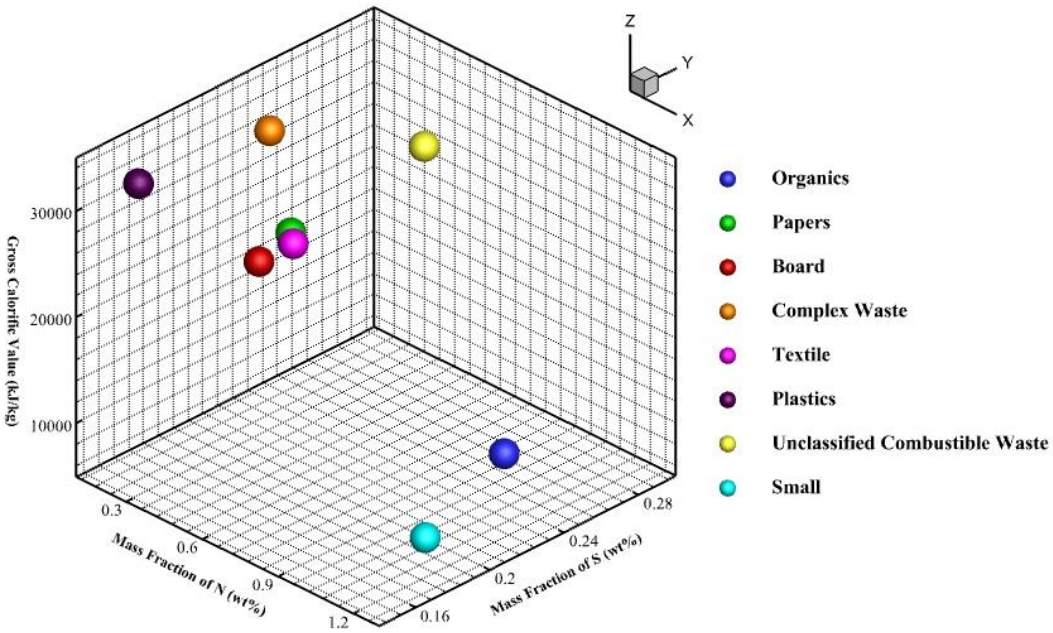

Figure. 9. Graph of Nitrogen and Sulphur vs Gross Calorific Value.

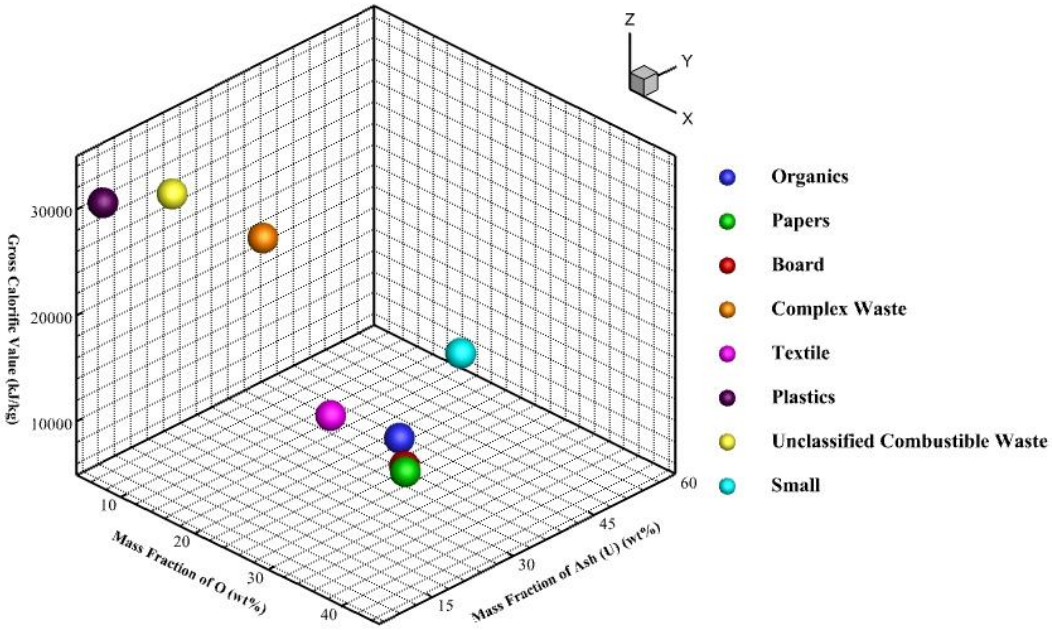

Figure. 10. Graph of Oxygen and Ash Content vs Gross Calorific Value.

Based on data shown in Figure 10, indicates an inverse relationship between oxygen content and ash content with gross calorific value, suggesting that materials with high oxygen and ash content tend to have lower gross calorific values. Plastics with very low oxygen and relatively low ash content demonstrate the highest gross calorific values due to their dominant hydrocarbon proportion. Conversely, the calorific value of small particles with high ash percentages is lowest because the presence of non-combustible inorganic materials dilutes the energy-carrying material, thereby increasing the heat capacity and thermal mass that absorbs heat during combustion. Consequently, the combustion temperature and energy conversion efficiency undergo a decline. In practice, it is necessary to separate and reduce the ash fraction and dry it so that the hydrocarbon-rich fraction is evaluated on a dry mass basis. This approach allows for the attainment of a more representative estimate of energy potential and the reduction of the necessity for emission control. Paper and board exhibit relatively high oxygen but moderate ash content, resulting in an intermediate heat value, thereby confirming that oxygen is not the only factor determining actual energy. From a chemical perspective, the presence of oxygen in molecules serves to reduce the number of carbon and hydrogen atoms that can undergo

oxidation. This, in turn, leads to a reduction in the chemical energy that is released. Furthermore, the presence of oxygen groups has been observed to enhance the rates of devolatilization and volatility, thereby facilitating more expeditious combustion processes without concomitant increases in the maximum available energy. In real-world settings, this can lead to an increase in heat loss and the formation of substandard products, consequently reducing the usable calorific value.

C. Proximate Anlysis

The proximate analysis of MSW materials indicates a significant correlation between volatile matter content, ash content, and gross calorific value. As demonstrated in Table 9, the presence of high volatile matter alongside low ash content results in an elevated GCV, as evidenced by the example of plastics, which contain approximately 90% volatile matter and negligible ash, yielding a GCV at 30,314.031 kJ/kg. Conversely, complex waste with elevated levels of volatile matter demonstrates the highest GCV, measured at 31,588.693 kJ/kg. Conversely, small waste fractions measuring between 8 and 20 millimeters contain approximately 60% ash and minimal volatile matter, yielding the lowest GCV at 6,654.604 kJ/kg. Paper and board materials are classified as mid-range materials, exhibiting approximately 72% volatile matter and moderate ash levels, resulting in a GCV ranging from 17,906.940 to 18,104.381 kJ/kg. The organic fraction, characterized by moderate volatile matter and a relatively high ash content, exhibits a lower GCV at 13,382.879 kJ/kg. The reduction of the ash fraction and the separation of volatile-rich materials are pivotal steps in enhancing the energy potential of MSW.

TABLE 9.
PROXIMATE ANALYSIS AND GROSS CALORIFIC VALUE

Category	Thermal Characteristics (wt%)			GCV (kJ/kg)
	VM	Ash (P)	FC	
Organics	54.410	26.328	19.262	13382.879
Papers	73.500	10.752	15.748	18104.381
Board	72.641	12.229	15.130	17906.940
Complex Waste	78.265	14.165	7.570	31588.693
Textile	79.829	6.546	13.625	21851.074
Plastics	89.989	8.376	1.635	30314.031
Unclassified Combustible Waste	78.619	20.197	1.184	28428.064
Small (8-20 mm)	32.696	60.579	6.725	6654.604

Volatile matter and fixed carbon are combustible components; however, ash does not provide energy. Volatile matter carries a fraction of hydrocarbons that are easily devolatilized and produce rapid heat release during combustion. Therefore, the higher the volatile matter, the greater the potential GCV, provided that the combustion process is able to completely oxidize the volatiles according to the principles of proximate analysis and devolatilization kinetics. Fixed carbon contributes energy through the combustion of residual charcoal after devolatilization, thereby increasing the GCV on an ash-free dry basis. This is due to the fact that a high fixed carbon fraction adds to the continuous heat release during the pyrolytic and oxidative combustion stages. Ash functions as an inorganic compound that serves to dilute the energy-bearing material and absorb heat due to its superior heat capacity. Consequently, as the ash content increases, the gross calorific value per kilogram decreases in accordance with the principles of mass and energy conservation. Furthermore, the presence of excessively high volatile matter in the absence of adequate combustion conditions has been demonstrated to increase the risk of incomplete combustion and heat loss, thereby reducing the true calorific value. Consequently, GCV evaluation is required to be conducted on a dry, ash-free mass basis, accompanied by an analysis of the balance between volatile matter, fixed carbon, and ash. This analysis is essential for the design of pre-separation drying and combustion parameters that ensure complete combustion of volatiles and minimize ash.

IV. CONCLUSION

The present study investigated the gasification suitability of municipal waste fractions through a combination of ultimate and proximate analysis, as well as bomb calorimetry. The findings indicated a robust positive correlation between carbon and hydrogen content with gross calorific value, while oxygen, nitrogen, sulphur, and ash exhibited negative impacts. The presence of volatile matter and fixed carbon has been shown to enhance the release of energy. However, a high ash content has been observed to diminish fuel quality and heat retention. Plastics and complex waste exhibited the highest GCV, ranging from 30,000 to 31,600 kJ/kg, while the small fraction demonstrated the lowest, ranging from 6,600 kJ/kg. The variability in composition necessitates meticulous feedstock management in reactor design. Effective pretreatments, such as drying and sorting, are essential, and GCV reporting must be on an ash-free dry basis for accurate emissions estimates. It is recommended that subsequent research endeavor to explore seasonal variations and incorporate gasification performance testing at the experimental scale to validate field data projections.

REFERENCES

[1] Badan Pusat Statistik Indonesia, "Penduduk, Laju Pertumbuhan Penduduk, Distribusi Persentase Penduduk, Kepadatan Penduduk, Rasio Jenis Kelamin Penduduk Menurut Provinsi, 2022." Accessed: Aug. 01, 2025. [Online]. Available: https://www.bps.go.id/id/statistics-table/3/V1ZSbFRUY3lTbFpEYTNsVWNGcDZjek53YkhsNFFUMDkjMw==/penduduk-laju-pertumbuhan-penduduk-distribusi-persentase-penduduk-kepadatan-penduduk-rasio-jenis-kelamin-penduduk-menurut-provinsi.html?year=2024

[2] International Energy Agency, "Indonesia - Countries & Regions." Accessed: Aug. 01, 2025. [Online]. Available: https://www.iea.org/countries/indonesia/emissions

[3] PT. Perusahaan Listrik Negara, "Rencana Usaha Penyediaan Tenaga Listrik (RUPTL) 2025–2034." Accessed: Aug. 08, 2025. [Online]. Available: https://gatrik.esdm.go.id/assets/uploads/download_index/files/b967d-ruptl-pln-2025-2034-pub-.pdf

[4] Badan Strategi Kebijakan Dalam Negeri, "Riset: 24 Persen Sampah di Indonesia Masih Tak Terkelola." Accessed: Aug. 01, 2025. [Online]. Available: https://bskdn.kemendagri.go.id/website/riset-24-persen-sampah-di-indonesia-masih-tak-terkelola/

[5] H. Li et al., "Expanding plastics recycling technologies: chemical aspects, technology status and challenges," Green Chemistry, vol. 24, no. 23, pp. 8899–9002, Nov. 2022, doi: 10.1039/D2GC02588D.

[6] National Academies of Sciences, Reckoning with the U.S. Role in Global Ocean Plastic Waste. 2021. doi: 10.17226/26132.

[7] "SIPSN - Sistem Informasi Pengelolaan Sampah Nasional." Accessed: Oct. 23, 2025. [Online]. Available: https://sipsn.kemenlh.go.id/sipsn/public/data/komposisi

[8] T. Suryanti, P. Setyono, and A. H. Ramelan, "Pengelolaan Sampah Kota Surakarta Dengan Data Mining," in PROSIDING SEMINAR NASIONAL SAINS DATA, 2024, pp. 411–420. doi: 10.33005/senada.v4i1.237.

[9] D. Porshnov, "Evolution of pyrolysis and gasification as waste to energy tools for low carbon economy," Wiley Interdiscip Rev Energy Environ, vol. 11, no. 1, Jan. 2022, doi: 10.1002/WENE.421.

[10] M. A. Satiada and A. Calderon, "Comparative analysis of existing waste-to-energy reference plants for municipal solid waste," Cleaner Environmental Systems, vol. 3, p. 100063, Dec. 2021, doi: 10.1016/J.CESYS.2021.100063.

[11] M. S. Abbas-Abadi et al., "Challenges and opportunities of light olefin production via thermal and catalytic pyrolysis of end-of-life polyolefins: Towards full recyclability," Prog Energy Combust Sci, vol. 96, p. 101046, May 2023, doi: 10.1016/J.PECS.2022.101046.

[12] O. Dogu et al., "The chemistry of chemical recycling of solid plastic waste via pyrolysis and gasification: State-of-the-art, challenges, and future directions," Prog Energy Combust Sci, vol. 84, p. 100901, May 2021, doi: 10.1016/J.PECS.2020.100901.

[13] H. H. Shah et al., "A review on gasification and pyrolysis of waste plastics," Front Chem, vol. 10, p. 960894, Feb. 2023, doi: 10.3389/FCHEM.2022.960894/XML.

[14] "PP No. 79 Tahun 2014." Accessed: Mar. 11, 2025. [Online]. Available: https://peraturan.bpk.go.id/Details/5523/pp-no-79-tahun-2014

[15] S. Gerassimidou, C. A. Velis, and D. Komilis, "Establishing a sub-sampling plan for waste-derived solid recovered fuels (SRF): Effects of shredding on representative sample preparation based on theory of sampling (ToS)," Waste Management, vol. 113, pp. 430–438, Jul. 2020, doi: 10.1016/J.WASMAN.2020.06.010.

[16] "ASTM D6051-15(2023) - Guide for Composite Sampling and Field Subsampling for Environmental Waste Management Activities," Apr. 01, 2023, ASTM International, West Conshohocken, PA. doi: 10.1520/D6051-15R23.

[17] S. Gerassimidou, C. A. Velis, R. A. Bourne, D. Komilis, E. Garcia-Taengua, and P. T. Williams, "Statistical quantification of sub-sampling representativeness and uncertainty for waste-derived solid recovered fuel (SRF): Comparison with theory of sampling (ToS)," J Hazard Mater, vol. 388, Apr. 2020, doi: 10.1016/j.jhazmat.2019.122013.

[18] K. Khodier et al., "Sampling and analysis of coarsely shredded mixed commercial waste. Part I: procedure, particle size and sorting analysis," International Journal of Environmental Science and Technology 2019 17:2, vol. 17, no. 2, pp. 959–972, Sep. 2019, doi: 10.1007/S13762-019-02526-W.

[19] M. Wasserman, M. Anshassi, and T. G. Townsend, "Assessing Sample Number Requirements for Municipal Solid Waste Composition Studies," J Hazard Toxic Radioact Waste, vol. 26, no. 1, p. 04021038, Jan. 2022, doi: 10.1061/(ASCE)HZ.2153-5515.0000652.

[20] "ASTM D5373-16 - Standard Test Methods for Determination of Carbon, Hydrogen and Nitrogen in Analysis Samples of Coal and Carbon in Analysis Samples of Coal and Coke," Sep. 01, 2016, ASTM International, West Conshohocken, PA. doi: 10.1520/D5373-16.

[21] "ASTM D4239-18 - Standard Test Method for Sulfur in the Analysis Sample of Coal and Coke Using High-Temperature Tube Furnace Combustion," Sep. 01, 2018, ASTM International, West Conshohocken, PA. doi: 10.1520/D4239-18.

[22] J. Speight, Biomass processes and chemicals. 2022. Accessed: Nov. 01, 2025. [Online]. Available: https://books.google.com/books?hl=en&lr=&id=CYVTEAAAQBAJ&oi=fnd&pg=PP1&dq=Biomass+Processes+and+Chemicals+James+G.+Speight&ots=J8QVIMquK-&sig=k9BVLabtHSoYzgDzionOjSIyIrI

[23] J. B. Trombley, C. Wang, and S. N. Thennadil, "Model-free measurements of calorific content and ash content of mixed garden wastes using a bomb calorimeter," Fuel, vol. 352, p. 129105, Nov. 2023, doi: 10.1016/J.FUEL.2023.129105.

[24] "ASTM D3173M-17a - Standard Test Method for Moisture in the Analysis Sample of Coal and Coke," Aug. 01, 2017, ASTM International, West Conshohocken, PA. doi: 10.1520/D3173_D3173M-17A.

[25] Y.-H. Kiang, "Basic properties of fuels, biomass, refuse derived fuels, wastes, biosludge, and biocarbons," Fuel Property Estimation and Combustion Process Characterization, pp. 41–65, 2018, doi: 10.1016/B978-0-12-813473-3.00003-9.

[26] X. Chen et al., "Moisture content effects on self-heating in stored biomass: An experimental study," Energy, vol. 285, p. 129391, Dec. 2023, doi: 10.1016/J.ENERGY.2023.129391.

[27] A. Price-Allison et al., "The Impact of Fuelwood Moisture Content on the Emission of Gaseous and Particulate Pollutants from a Wood Stove," Combustion Science and Technology, vol. 195, no. 1, pp. 133–152, Jan. 2023, doi: 10.1080/00102202.2021.1938559.

[28] B. S. Adeboye, M. O. Idris, W. O. Adedeji, A. A. Adefajo, T. F. Oyewusi, and A. Adelekun, "Characterization and energy potential of municipal solid waste in Osogbo metropolis," Cleaner Waste Systems, vol. 2, p. 100020, Jul. 2022, doi: 10.1016/J.CLWAS.2022.100020.

[29] "ASTM D3174-12(2018)e1 - Test Method for Ash in the Analysis Sample of Coal and Coke from Coal," Oct. 15, 2018, ASTM International, West Conshohocken, PA. doi: 10.1520/D3174-12R18E01.

[30] "ASTM D3175-18 - Standard Test Method for Volatile Matter in the Analysis Sample of Coal and Coke," Dec. 01, 2018, ASTM International, West Conshohocken, PA. doi: 10.1520/D3175-18.

[31] "ASTM D3172-13 - Standard Practice for Proximate Analysis of Coal and Coke," Apr. 01, 2021, ASTM International, West Conshohocken, PA. doi: 10.1520/D3172-13R21E01.

[32] "ASTM D5865/D5865M-19 - Test Method for Gross Calorific Value of Coal and Coke," Jun. 01, 2019, ASTM International, West Conshohocken, PA. doi: 10.1520/D5865_D5865M-19.

[33] "ASTM D1857M-18 - Standard Method for Fusibility of Coal and Coke Ash," Sep. 01, 2018, ASTM International, West Conshohocken, PA. doi: 10.1520/D1857_D1857M-18.

[34] H. J. Sinaga, "ANALISIS PERBANDINGAN PENENTUAN PERINGKAT BATUBARA ANTARA REKLEKTAN VITRINIT DAN ANALISIS LAIN DIDAERAH X," Jurnal Eksakta Kebumian, vol. 2, no. 1, pp. 7–13, 2021, Accessed: Sep. 23, 2025. [Online]. Available: https://e-journal.trisakti.ac.id/index.php/jek/article/view/16569

[35] S. S. SHAPIRO and M. B. WILK, "An analysis of variance test for normality (complete samples)," Biometrika, vol. 52, no. 3–4, pp. 591–611, Dec. 1965, doi: 10.1093/BIOMET/52.3-4.591.

[36] L. H, "Robust tests for equality of variances," Contributions to probability and statistics, pp. 278–292, 1960, Accessed: Oct. 02,

2025. [Online]. Available: https://cir.nii.ac.jp/crid/1573950400526848896

[37] B. L. Welch, "On the Comparison of Several Mean Values: An Alternative Approach," Biometrika, vol. 38, no. 3/4, p. 330, Dec. 1951, doi: 10.2307/2332579.

[38] M. B. Brown and A. B. Forsythe, "Robust Tests for the Equality of Variances," J Am Stat Assoc, vol. 69, no. 346, pp. 364–367, 1974, doi: 10.1080/01621459.1974.10482955.

[39] M. Bird, C. Keitel, and W. Meredith, "Analysis of biochars for C,H,N,O and S by elemental analyser," 2017.

[40] J. C. Brown, "ENERGY | Measurement of Food Energy," Encyclopedia of Food Sciences and Nutrition, pp. 2087–2091, Jan. 2003, doi: 10.1016/B0-12-227055-X/00406-5.